



OPEN ACCESS

EDITED BY

Siti R. Yusof,
Universiti Sains Malaysia (USM), Malaysia

REVIEWED BY

Anuska V. Andjelkovic,
University of Michigan, United States
Abraham Jacob Al-Ahmad,
Texas Tech University Health Sciences
Center, United States

*CORRESPONDENCE

Andrea E. Toth,
✉ tandinak@gmail.com
Morten S. Nielsen,
✉ mn@biomed.au.dk

SPECIALTY SECTION

This article was submitted to CNS Drug
Delivery,
a section of the journal
Frontiers in Drug Delivery

RECEIVED 28 October 2022

ACCEPTED 20 December 2022

PUBLISHED 05 January 2023

CITATION

Toth AE, Klepe A, Lipka DV, Goldman C,
Brodin B and Nielsen MS (2023), SorLA in
astrocytes regulates blood-brain
barrier integrity.
Front. Drug. Deliv. 2:1082689.
doi: 10.3389/fddev.2022.1082689

COPYRIGHT

© 2023 Toth, Klepe, Lipka, Goldman,
Brodin and Nielsen. This is an open-access
article distributed under the terms of the
[Creative Commons Attribution License
\(CC BY\)](https://creativecommons.org/licenses/by/4.0/). The use, distribution or
reproduction in other forums is permitted,
provided the original author(s) and the
copyright owner(s) are credited and that
the original publication in this journal is
cited, in accordance with accepted
academic practice. No use, distribution or
reproduction is permitted which does not
comply with these terms.

SorLA in astrocytes regulates blood-brain barrier integrity

Andrea E. Toth^{1*}, Adrian Klepe¹, Dora V. Lipka¹,
Charlotte Goldman², Birger Brodin² and Morten S. Nielsen^{1*}

¹Department of Biomedicine, Faculty of Health, Aarhus University, Aarhus, Denmark, ²Department of Pharmacy, Faculty of Health and Medical Sciences, University of Copenhagen, Copenhagen, Denmark

The brain's homeostasis depends heavily on the integrity of the blood-brain barrier (BBB). Astrocytes are an essential part of the BBB in modulating and maintaining the barrier properties of the brain endothelial cells (BECs). Despite decades of research, the elements of glial regulation are not fully elucidated. SorLA/SorL1/LR11, a multifunctional receptor, is the most composite member of the Vps10p domain receptor family. In this study, we characterize the expression and function of SorLA in the cells of the BBB. The applied *in vitro* approaches describe BBB functions in primary cells isolated from wild-type and *Sorl1*^{-/-} knock-out rats. Here, we present that *Sorl1* gene is highly expressed in wild-type astrocytes but not in BECs and pericytes. Furthermore, we show that SorLA in astrocytes is an important regulator of the BBB's tightness. The primary rat BBB models where astrocytes lack SorLA protein proved leaky, which correlated well with the decrease in claudin-5 tight junction protein in BECs. Meanwhile, other junctional proteins, i.e., occludin and zonula occludens-1 are unaffected. Collectively, these data suggest that the absence of SorLA in astrocytes affects the tight junctions of BECs, thereby disturbing the BBB. Our results add another layer to understanding astrocyte-endothelial interactions in the healthy and diseased BBB.

KEYWORDS

SorLA, SorL1, LR11, astrocytes, blood-brain barrier, claudin-5, tight junction, brain endothelial cells

1 Introduction

Recently, the vacuolar protein sorting 10 protein domain (Vps10p-D) receptor family has received much attention due to their fundamental role in health and diseases (Andersen et al., 2006; Malik and Willnow, 2020). SorL1 or SorLA (sorting protein-related receptor containing low-density lipoprotein (LDL) receptor class A repeats) is a member of this receptor family. Besides the Vps10p-D, SorLA contains structural elements of the LDL receptor family; therefore, it is also called lipoprotein receptor 11 (LR11) (Jacobsen et al., 1996; Yamazaki et al., 1996). SorLA is a multifunctional receptor that interacts with various cargo proteins and mediates their intracellular localization, lysosomal degradation, or secretion. The cytoplasmic domain of the receptor binds AP-1, AP-2, the retromer complexes, and other cytosolic adaptors that mediate

Abbreviations: BBB, blood-brain barrier; BECs, brain endothelial cells; DMEM, Dulbecco's Modified Eagle Medium; GFAP, glial fibrillary acidic protein; KO, *Sorl1*^{-/-} knock-out; KO-BBB, *in vitro* BBB model where KO-BECs are co-cultured with KO-astrocytes; LDL, low-density lipoprotein; LR11, lipoprotein receptor 11; Mixed-BBB, mixed genotypic *in vitro* BBB model where WT-BECs are co-cultured with KO-astrocytes; P_{app}, apparent permeability coefficient; PBS, phosphate buffer saline; RT-qPCR, Real-time quantitative PCR; SorLA, sorting protein-related receptor containing low-density lipoprotein (LDL) receptor class A; TEER, transendothelial electrical resistance; Vps10p-D, vacuolar protein sorting 10 protein domain; WT, wild-type; WT-BBB, *in vitro* BBB model where WT-BECs are co-cultured with WT-astrocytes; ZO-1, zonula occludens-1.

the endocytosis and the intracellular endosome to Golgi network trafficking of the receptor and its ligand (Nielsen et al., 2007). SorLA-mediated sorting influences the amount and activities of several substrate proteins such as enzymes, neuropeptides, signaling receptors, and growth factors (for review, see (Malik and Willnow, 2020)). The activity of SorLA is vital for the proper molecular mechanism in cells, and dysfunction of the receptor can lead to devastating illnesses such as Alzheimer's disease (Andersen et al., 2016), cerebrovascular pathologies (Cuenco et al., 2008), atherosclerosis (Kanaki et al., 1999; Klinger et al., 2011), and obesity (Whittle et al., 2015; Schmidt et al., 2016). SorLA is abundantly expressed in the nervous system (Hermans-Borgmeyer et al., 1998; Motoi et al., 1999), and it has been investigated in neurons and in glial cells (Willnow et al., 2008). However, the function of SorLA at the blood-brain barrier (BBB) has not been addressed so far (Toth and Nielsen, 2023).

The BBB is a highly specialized structure of the brain capillaries, which regulates the exchange of gases and nutrients between the blood and the brain. It furthermore protects the brain from toxic insults by blocking harmful agents' entry (Abbott et al., 2010). Brain endothelial cells (BECs) form the anatomical basis of BBB, closely tied to each other with tight and adherent junctions. These complexes are built from highly specialized transmembrane receptors and their cytoplasmic linker proteins (Stamatovic et al., 2016). Occludin and claudin-5 are two of the major constitutive transmembrane proteins in the tight junctions of the BBB (Ohtsuki et al., 2008). Both transmembrane proteins are linked intracellularly to a number of regulatory scaffolding proteins, such as the zonula occludens-1 (ZO-1) protein (Fanning et al., 1998; Itoh et al., 1999). The BECs of the BBB constantly communicate with other cells of the brain. Astrocytes, pericytes, microglia, and neurons enable the BECs to develop and maintain unique barrier properties (Abbott et al., 2010). Many studies emphasize that the interaction between the BECs and astrocytes is crucial for barrier function, where particular astrocyte-released agents targeting distinct receptors at the BEC have been demonstrated to possess an extensive repertoire of possibilities for complex responses (Alvarez et al., 2013). The crosstalk between these cells upregulates unique BBB features in BECs (Janzer and Raff, 1987), e.g., low permeability (Dehouck et al., 1990), and high transendothelial electrical resistance (TEER) (Rubin et al., 1991), along with a specific arrangement of tight junction proteins (Hamm et al., 2004). The brain's homeostasis heavily depends on the tightness of the junctions between the BECs. Under pathological conditions, malfunctions of tight junctions lead to neuronal damage and, finally, to the development of diseases (Stamatovic et al., 2016). Despite several years of research, the complete repertoire of factors and signaling pathways for maintaining and modulating the integrity of the BBB is not entirely elucidated. Recently, sortilin, another member of the Vps10p-D family, has been reported to play an essential role in regulating the BBB's integrity (Toth et al., 2022). Here, we focus on another member of this receptor family, SorLA.

This work aims to describe the expression of SorLA in the cells of the BBB, including astrocytes, BECs, and pericytes, and to elucidate its potential involvement in maintaining the integrity of the BBB.

2 Materials and methods

2.1 Materials

All chemicals and reagents were purchased from Merck (Soeborg, Denmark.) unless otherwise indicated.

2.2 Animals

Wild-type (WT) Sprague Dawley rats were purchased from Janvier Labs. The *Sorl1*^{-/-} (KO) Sprague Dawley rats were custom-made by Horizon Discovery for breeding at the Animal Facility at Aarhus University. *Sorl1*^{-/-} has a seven base pair deletion in exon 3, resulting in a stop codon which leads to the subsequent complete destruction of the Vps10p-D folding in the SorLA protein. No mRNA splice variants or protein fragments were detected by RT-PCR or Western blot analysis. The KO-rats were kept in standard cages (Scanbur) in a pathogen-free and temperature-controlled environment. Cages were cleaned weekly and supplied with nesting and bedding material, a wooden stick, and a tunnel. Chow (Altromin 1324, Brogaarden, Denmark) and water were provided *ad libitum*. The light was provided during daytime in 12 h light/12 h dark cycle. Animals were treated according to the European and Danish animal experimentation legislation (directive 2010/63/EU). Animal experiments were permitted by the Danish Animal Experiments Inspectorate under permission number 2017-15-0201-01192.

2.3 Primary cell culture isolations

Primary BECs, astrocytes, and pericytes were isolated and cultured, as reported previously (Nakagawa et al., 2009; Toth et al., 2022). For BECs and pericytes, cell cultures of brain microvessels were isolated from the forebrain of 3-week-old rats. The meninges were removed, and the grey matter was minced into small pieces. 1 mg/ml collagenase CLS2 (Worthington, United States) in Dulbecco's modified Eagle medium (DMEM) for 1.5 h at 37°C was used for tissue digestion. The myelin contamination was removed by centrifugation (1,000×g, 20 min) in 20% bovine serum albumin–DMEM. The remaining microvessels were further digested with 1 mg/ml collagenase-dispase (Roche) in DMEM for 1 h. Brain capillaries were separated on a 33% continuous Percoll gradient (1,000×g, 10 min) and collected. The isolated microvessels were frozen in 10% dimethyl sulfoxide - fetal bovine serum mixture until further use.

Brain microvessel fragments contain pericytes as well as BECs. The survival and proliferation of the pericytes were ensured by specific culture conditions. Pericytes typically overgrow BECs during 2 weeks of culturing in DMEM supplemented with 10% FBS and antibiotics in uncoated culture dishes. (Nakagawa et al., 2007). The culture medium was changed twice a week.

Cultures of astrocytes were prepared from 1–2 days-old newborn rats. The brains were mechanically dissociated into cortical pieces and plated in poly-L-lysine coated T75 flasks (Thermo Fisher Scientific, Roskilde, Denmark). The cells were grown for a minimum of 3 weeks in DMEM containing 1% penicillin/streptomycin, and 10% FBS. The culture was shaken and washed with phosphate buffered saline (PBS) twice a week to remove contaminating microglia. After 3 weeks, astrocytes were frozen 10% dimethyl sulfoxide - fetal bovine serum mixture until further use. Before co-culture, astrocytes were thawed and grown as in 12-well plate. In 2 weeks, the culture became confluent, and the medium was changed every 3 days from now on.

2.4 *In vitro* BBB models

For BECs, T75 flasks were coated with collagen IV (100 µg/ml) and fibronectin (100 µg/ml) 10% plasma-derived bovine serum (First Link

Ltd., Wolverhampton, United Kingdom). Basic fibroblast growth factor (1 ng/ml), heparin (15U), insulin-transferrin-selenium, and gentamicin (5 µg/ml) were added to the DMEM/F12 medium. To the media of the towed rat brain capillaries, puromycin (4 µg/ml) was supplemented for the first 4 days to obtain a pure culture of BECs and remove contaminating cells. On the fifth day, the cells were passaged onto 1.12 cm² polycarbonate Transwell® filter inserts with .4 µm pore size (Costar, Corning, Kennebunk, ME, United States) at a density of 1 × 10⁵ cells/cm². On the following day, the non-contact co-culture BBB models were established. The inserts of the BECs were placed in the 12-well culture dishes of astrocytes. On the third day of co-culture, media of BECs and astrocytes were supplied with differentiation factors: 550 nM hydrocortisone, 250 µM 8-(4-chlorophenylthio) adenosine-3',5'-cyclic monophosphate (cAMP) and 17.5 µM RO-201724. On the next day, permeability experiments were carried out, and the samples were collected for further investigation. The tightness of the *in vitro* BBB models was checked visually and by measuring TEER.

This study used three different models: WT-BBB, KO-BBB, and a mixed genotypic BBB model (mixed-BBB). The WT-BBB model was used as a control, which contained WT-BECs on the top of WT-astrocytes. Similarly, in the KO-BBB model, KO-BECs were co-cultured with KO-astrocytes. For the mixed-BBB model, the inserts of the WT-BECs were placed on top of KO-astrocytes. The mixed- or the KO-models were created and maintained parallelly with the WT-BBB model. All the cell cultures and BBB models were held in a humidified incubator with 5% CO₂ at 37°C.

2.5 Real-time quantitative PCR (RT-qPCR)

Astrocytes and pericytes were cultured in T75 flasks while BECs were grown on 75 mm diameter polycarbonate Transwell® inserts (Costar, Corning) in co-culture with astrocytes as described in '*In vitro* BBB models'. Before harvesting all the cell cultures, they were washed twice with ice-cold PBS. NucleoSpin® RNA Isolation Kit (Macherey-Nagel, Düren, Germany) was used to extract total RNA by following the manufacturer's instructions. Material from one insert or one T75 flask was used to generate each RNA sample, and the cells for the 3 parallel samples originate from 3 different cell isolations. NanoDrop 2000c UV-VIS Spectrophotometer (ThermoFisher Scientific, Waltham, MA, United States) was used to measure mRNA purity. For further analysis, mRNA samples with a 260/280 ratio over 2.00 were used. SDCS BiologyWorkbench and NCBI retrieved from Thermo Fisher Scientific were used to design primers. To perform reverse transcription of mRNA, High capacity cDNA reverse transcription kit (4368814; from Thermo Fisher Scientific) was used according to the manufacturer's protocol. For reverse transcription of mRNA to cDNA, PTC-200 ThermalCycler (MJ Research) was applied with Riboloc R1 (Thermo Scientific) RNase inhibitor. The following primer pairs were used: SorLA fwd 5'-AAGGTGCACAACACCAATGA-3', rvs 5'-GTGCCCAAGAATCACACCTT-3', product size 117 bps; Glyceraldehyde-3-Phosphate Dehydrogenase (GAPDH) fwd 5'-AGACAGCCGCATCTTCTTGT-3', rvs 5'-CTTGCCGTGGGTAGAGTCAT-3', product size 207 bps; β-actin fwd 5'-TGTCACCAACTGGGACGATA-3', rvs 5'-CTGGGTCATCTTTTCACGGT-3', product size 139 bps. Primer efficiencies were calculated by the equation $E = 10^{-1/\text{slope}}$. The slope was created from a ten-fold serial dilutions calibration curve. All the primer pairs have regular melting curves, and

their efficiency range was between 1.9 and 2.1. Light Cycler 96 Instrument (Roche, Basel, Switzerland) was used for the RT-qPCR analysis. The used amount of cDNA corresponds to .31 µg RNA per reaction. 20 µl reaction mixture consisted of 2 µl cDNA, 5 µl primer (a mix containing 2 µM of forward and reverse primers), 3 µl water (PCR-grade), and 10 µl mastermix. Cycling conditions were as follows: pre-incubation at 95°C for 600 s, 45 cycles 95°C for 10 s, 55°C for 10 s, and 72°C for 20 s. To verify the specificity of amplicons, melting curves were determined for all samples. All samples were run in triplicates. All PCR data were normalized to the geomean of reference genes of β-actin and GAPDH. Genes were considered not to be expressed above 35 average cycle-threshold value.

2.6 Western blot

Cell lysates was prepared by washing the cells three times in PBS and lysed in ExB lysis buffer (150 mM NaCl, 20 mM MgCl₂, 20 mM CaCl₂, 100 mM HEPES, 1% TritonX-100, complete™ protease inhibitor). From each cell lysate a minimum of 5 µg of was loaded on a 4–12% polyacrylamide gel (GeneScript, New Jersey, United States). The protein samples were transferred to a nitrocellulose membrane (Invitrogen iBlot) and the membrane was blocked in 5% skimmed milk, .01 M Tris-HCl, .15 M NaCl, and .1% Tween 20, pH 7.6 in buffer solution and incubated with primary antibodies overnight at 4°C. For primary antibodies, mouse anti-LR11 (SorLA) antibody (612,633, 1:1,000, B.D. Transduction Laboratories San Diego, CA, United States) and mouse anti-β-actin antibody (A5441, 1:1,000) were used. Next, the samples were treated with secondary horseradish peroxidase-conjugated anti-mouse IgG antibodies (1:2000) for 1 h at room temperature. The bands were detected using ECL (G.E. Healthcare) or SuperSignal (Thermo Scientific, Rockford, United States) according to the manufacturer's protocol and visualized using LAS 4000 (Fujifilm). To improve clarity for representative Western blot images, contrast and brightness adjustment were applied equally across the entire picture.

2.7 Measurement of tightness and permeability

EVOM resistance meter using EndOhm-12 cup system (World Precision Instruments Inc, Sarasota, FL, United States) was used to measure TEER. TEER values were calculated relative to the surface area ($\Omega \times \text{cm}^2$) and shown in each experiment as a percentage of the WT-group.

To evaluate the permeability across endothelial cell layers, a small molecular weight marker, sodium fluorescein (376 Da) was used. BECs have grown to a confluency of 100% on Transwell inserts as described above. For the permeability experiments, the culture medium was replaced by DMEM phenol red-free medium (Gibco, Life technologies). In the upper chambers (luminal compartment) the 500 ml medium was supplemented with 10 µg/ml sodium fluorescein and 1% bovine serum albumin. The abluminal (lower) compartment contained the 1.5 ml medium without any supplements. The plates were gently shaken (150 rpm) on a horizontal shaker in a 37°C incubator with 5% CO₂. To minimize luminal to abluminal transport, every 20 min the inserts were transferred to a new well for 1 h. The concentrations of the marker molecules in samples from the abluminal (lower) compartments were determined by fluorescent spectrophotometry (emission: 525 nm,

excitation: 440 nm) with Enspire multimode plate reader (PerkinElmer Inc., Lillestrøm, Norway). Flux across coated inserts without cells was also measured. The apparent permeability coefficient (P_{app}) was calculated by the following equation (Youdim et al., 2003).

$$P_{app} \left(\frac{\text{cm}}{\text{s}} \right) = \frac{\Delta[C]_A * V_A}{A * [C]_L * \Delta t}$$

$\Delta[C]_A$ —concentration difference of the tracer in the abluminal compartments at the end of the experiment.

V_A —volume of the abluminal compartment (1.5 ml).

A —surface area available for permeability (1.1 cm²).

$[C]_L$ —concentration of the tracer in the luminal compartments at beginning of the experiment.

Δt —length of the experiment (1 h).

The P_{app} values of the samples are compared in each experiment to mean value of the WT-group and shown as its percentage.

2.8 Immunocytochemistry and confocal microscopy

For immunostaining, astrocytes were grown on coated cover glasses while BECs were cultured on polycarbonate Transwell® filter inserts in co-culture with astrocytes as described above. All steps of immunocytochemistry were carried out at room temperature. Confluent cell layers were fixed with 4% paraformaldehyde in PBS for 20 min. The samples were permeabilized in .2% Triton X-100 in PBS for 10 min and blocked in 2% bovine serum albumin in PBS for 20 min. Primary and secondary antibodies were diluted in 1.5% bovine serum albumin and .05% Triton X-100. The following primary antibodies were applied for 1 h: mouse anti-LR11 antibody (612,633, 1:300 BD Transduction Laboratories), rabbit anti-claudin 5 antibody (SAB4502981, 1:300), rabbit anti-ZO-1 antibody (61–7300, 1:300; Invitrogen, Carlsbad, CA, United States), rabbit anti-occludin antibody (71–1,500, 1:300; ThermoFischer Scientific, Rockford, IL, United States), mouse anti-gial fibrillary acidic protein antibody (GA5; 3670, 1:200; Cell Signaling Technology, Danvers, MA, United States). The samples were treated with secondary antibodies (Alexa Fluor-488 conjugated anti-mouse (1:400) and Alexa Fluor-568 conjugated anti-mouse or anti-rabbit (1:400)) for 1 h. For nuclei staining, Hoechst 32,528 (.5 µg/ml) was diluted in distilled water and applied for 10 min as a separate step on the samples. To remove unbound antibodies, samples were washed three times for 5 min in .02% Triton-X100 in PBS in between the stages. As the last step, samples were mounted on glass slides with Dako fluorescence mounting medium (Dako, Glostrup, Denmark). Confocal images were taken using an inverted Olympus IX-83 fluorescent microscope with Yokogawa confocal spinning unit, and Andor iXon Ultra 897 camera, Olympus UPlanSApo, 60x/1.20 NA water lens. More than three images of randomly selected fields of each sample were acquired. On the compared representative images shown in this paper, the brightness and contrast adjustments were applied to the same extent in ImageJ software.

2.9 Line intensity scanning

Line intensity scan analysis was performed on images of BECs in Fiji software as described by Toth et al. (Toth et al., 2022). Minimum 3–5 cells were measured on each image by drawing lines in the

cytoplasm and the cell border. The intensity parameters were counted along the lines. At the cell border and in the cytoplasm, the measured fluorescent intensity values were compared between the WT- and the mixed-groups from the same experiment. The values are shown as a percentage of the WT-groups (100%) from each experiment.

2.10 Statistical analyses

All studies were conducted at least three times using a minimum of three samples for each group. All curve fitting and statistical analyses were performed in Graph Pad Prism version 7.0 (GraphPad Software, La Jolla, CA, United States). Values were compared using Student's t-test. Data are reported as means ± standard error of the mean (SEM). Changes were considered statistically significant at $p \leq .05$. Student's t-test was performed on the normalized data.

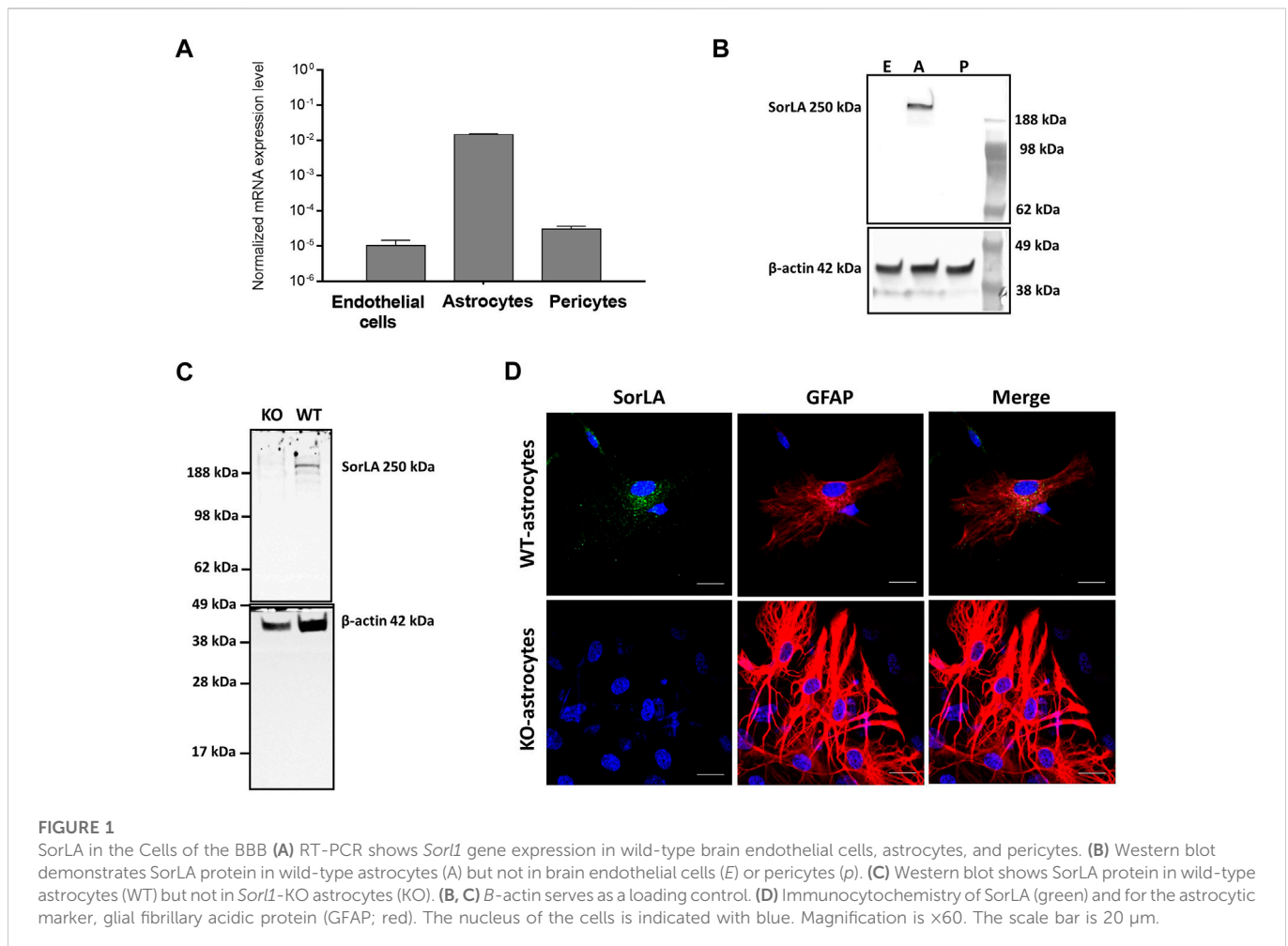
3 Results

3.1 SorLA in the cells of the BBB

To investigate what role SorLA plays at the BBB, we first analyzed the expression of *Sorl1* gene in the cell types constituting the brain capillaries from wild-type rats. The *Sorl1* gene was highly expressed in astrocytes. However, its expression level was negligibly low in BECs and pericytes (Figure 1A). To further validate *Sorl1* gene's expression, we investigated the protein level of SorLA in cultured BECs, astrocytes, and pericytes isolated from wild-type rats. In agreement with the gene expression data, Western blot showed that SorLA is present in the cell lysate of astrocytes, and it is not detectable in BECs and pericytes (Figure 1B). Accordingly, SorLA was only detectable in WT-, but not in KO-astrocytes (Figure 1C). As the next step, we characterized the subcellular localization of SorLA by immunocytochemistry (Figure 1D). Positive staining for SorLA could be observed only in the WT- and not in the KO-astrocytes. SorLA localized in vesicles of WT-astrocytes with a solid perinuclear placement. Both astrocytes expressed glial fibrillary acidic protein and showed a multipolar shape with long processes.

3.2 SorLA is involved in maintaining the BBB's integrity

Astrocytes play a vital role in maintaining the BBB's integrity. Therefore, we examined the tightness of the endothelial monolayer *in vitro* (Figure 2). As illustrated by Figure 2A, WT-BECs were co-cultured with WT-astrocytes; KO-BECs were maintained with KO-astrocytes. The TEER values reflect the tightness of the endothelial monolayer and indicate the permeability of the intercellular junctions for sodium ions (Srinivasan et al., 2015). The tightness of the KO-endothelial monolayer ($1,047 \pm 343 \Omega \times \text{cm}^2$) was three-fourth of the WT-endothelial monolayer's ($1,373 \pm 419 \Omega \times \text{cm}^2$) (Figure 2B). Accordingly, The KO-BBB model was leaky for sodium-fluorescein paracellular permeability marker (Figure 2C). We measured 1.7 times higher permeability ($3.41 \pm 1.49 \times 10^{-6} \text{ cm/s}$) across the KO-endothelial layer than across the WT-endothelial layer ($1.86 \pm .63 \times 10^{-6} \text{ cm/s}$).



SorLA is expressed only in astrocytes and not in BECs (Figures 1A, B). To prove that the KO-astrocytes compromise the integrity of the endothelial monolayers, we constructed a mixed-BBB model where WT-BECs were co-cultured with KO-astrocytes (Figure 2D). The tightness and permeability of the mixed models were similar to the KO-BBB models. The TEER values of the endothelial layer in the mixed-BBB model were 20% lower ($1,105 \pm 115 \Omega \times \text{cm}^2$) than the WT ones ($1,389 \pm 145 \Omega \times \text{cm}^2$) (Figure 2E). Accordingly, the measured permeability for sodium-fluorescein in the mixed-BBB model ($3.57 \pm 1.79 \times 10^{-6} \text{ cm/s}$) was 1.8 times higher than in the WT-BBB model ($1.86 \pm .63 \times 10^{-6} \text{ cm/s}$) (Figure 2F).

3.3 SorLA influences the tight junctions of the BECs

Since SorLA is expressed only in astrocytes (Figure 1), we continued to investigate how KO-astrocytes compromise the integrity of the barrier using the mixed BBB model. Altered tightness and permeability (Figures 2E, F) can indicate changes in the junctional proteins of the BECs (Lochhead et al., 2020). Therefore, we have investigated the localization of the most well-characterized tight junction proteins, namely claudin-5, occludin, and ZO-1 (Figure 3) in the BECs of mixed- and WT-BBB models (Figure 2D). At the cell border and in the cytoplasm, the

fluorescence intensity of the junctional proteins was measured to quantify the observed differences. The immunofluorescent staining of claudin-5 was weaker in the BECs of the mixed-BBB model (Figure 3A). Accordingly, the measured intensity values both at the cell border and in the cytoplasm were three-fourth of the BECs' from the WT-BBB model. The other two tight junction proteins also showed lower intensity in the mixed-BBB model. However, this change did not prove to be significant (Figures 3B, C). In any of the staining, we could not observe any morphological changes in the BEC when they were co-cultured with KO-astrocytes (Figure 3). Overall, the results indicated that a disturbance in claudin-5 caused the observed BBB leakage (Figure 2).

4 Discussion

SorLA has essential biological functions in the cells and tissues of the body and has been investigated intensively over the last 2 decades (Schmidt et al., 2017; Malik and Willnow, 2020). Since SorLA is abundantly expressed in the brain (Hermans-Borgmeyer et al., 1998; Kanaki et al., 1998; Motoi et al., 1999), its role in neurons and, to some degree, in glia cells of different brain regions has been described (Willnow et al., 2008). However, the microvessels of the brain forming the BBB have been neglected (Toth and Nielsen, 2023). Here, we investigated the presence of SorLA in the cells of the BBB on both gene

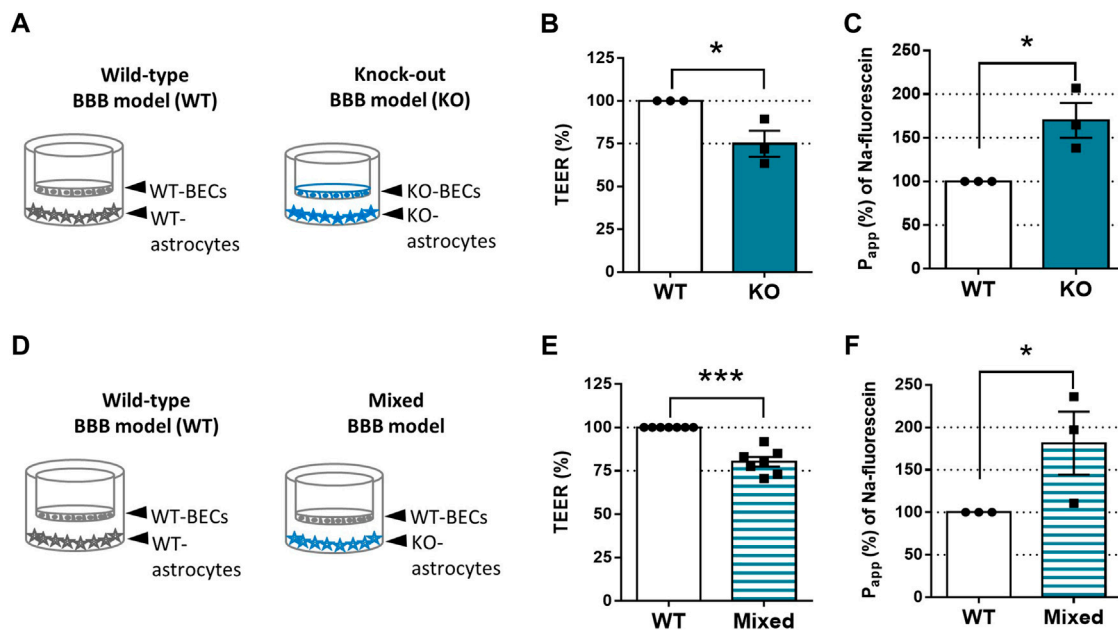


FIGURE 2

SorLA is Involved in Maintaining BBB's Integrity. (A) *In vitro* BBB model set-ups of Figures 2B, C. In the Wild-type (WT) BBB model, WT-brain endothelial cells (WT-BECs) were grown on permeable inserts in co-culture with WT-astrocytes at the bottom of the dish. In the same way in the KO-BBB model, KO-brain endothelial cells (KO-BECs) were kept together with KO-astrocytes. (B) Tightness (TEER) of KO-BBB model compared to the WT-BBB model. (C) Apparent permeability (P_{app}) for sodium-fluorescein of KO-BBB model compared to the WT-BBB model. (D) *In vitro* BBB model set-ups of Figures 2E, F. WT-BECs were grown on permeable inserts in a co-culture with WT-astrocytes at the bottom of the dish. In the same way in the mixed-BBB model, WT-BECs were kept together with KO-astrocytes. (E) Tightness (TEER) of KO-BBB model compared to the WT-BBB model. (F) Apparent permeability (P_{app}) for sodium-fluorescein of KO-BBB model compared to the WT-BBB model. Data are presented as mean \pm SEM $n \geq 3$ cultures. * $p \leq .05$, ** $p \leq .01$, *** $p \leq .001$ (Student's t-test).

expression and protein levels. We showed that SorLA is expressed and is detectable at a considerable protein level in astrocytes but not in BECs or pericytes. Previous wide-range gene expression studies from both mouse and human origins support our findings (Zhang et al., 2014b; Zhang et al., 2016; Vanlandewijck and Betsholtz, 2018a). They reported that *Sor1l* gene is expressed at a high level in astrocytes, but its expression is considerably lower in BECs and pericytes (Data ref: (Zhang et al., 2014a; Vanlandewijck and Betsholtz, 2018b)). Furthermore, our Western blot and immunocytochemistry data in primary rat astrocytes expand prior work in rat C6 glioma cell line (Salgado et al., 2012). We showed that SorLA is mainly localized in the soma of primary rat astrocytes, identical to the previous staining in C6 cell line (Salgado et al., 2012) and primary mouse astrocytes (Madsen et al., 2019). SorLA is a retrograde sorting receptor shuffling between the trans-Golgi network and the endosomes; therefore, the majority of the receptor can be found in the soma, near the nucleus, and only a small fraction on the cell surface (Jacobsen et al., 2001; Nielsen et al., 2007). Taken all together, we are the first to investigate SorLA's expression in the cells of the BBB on both gene expression and protein levels: We showed that SorLA is not expressed in primary BECs and pericytes isolated from rat microvessels. However, rat primary astrocytes express a considerable amount of the receptor.

Astrocytes are important regulators of the BBB's integrity (Dehouck et al., 1990; Rubin et al., 1991). Therefore, we have investigated the role of SorLA on the BBB *in vitro*. We used BBB models based on primary rat cells, as these have been proven to simulate the *in vivo* barrier concerning tightness, transporter activity,

and receptors (Helms et al., 2016). The KO-BBB model lacking SorLA proved paracellularly leaky and less tight than the WT-BBB model. To confirm that the KO-astrocytes compromise the integrity of the endothelial monolayers, we constructed a mixed-BBB model. In this model, only the astrocytes stemmed from KO-rats, and we co-cultured them with WT-BECs. The integrity of the mixed-BBB was compromised to the same extent as the KO-BBB model. The increased permeability and the lower TEER values of the mixed-BBB model proved that SorLA plays a vital role in the integrity of the BBB.

Altered tightness and permeability indicate changes in the junctions of the BECs (Lochhead et al., 2020). Therefore, we investigated the most well-characterized tight junction proteins, namely claudin-5, occludin, and ZO-1. Typically, most of these junctional proteins are localized at the cell border, giving intense fluorescent staining where the BECs attach to each other. In the cytoplasm, only a low level of proteins can be found (Stamatovic et al., 2016; Lochhead et al., 2020). Accordingly, we measured the fluorescence intensity of the proteins after immunocytochemistry using the line intensity scanning method at the cell border and in the cytoplasm. This method has been successfully used to quantify the observed differences in the localization of junctional proteins (Toth et al., 2022). The intensity of claudin-5's staining was weaker in the BECs which were co-cultured with astrocytes lacking SorLA. The degree of the intensity rate drop aligned well with the extent of the tightness and the permeability change in the mixed-BBB model. These results clearly indicate that a disturbance in claudin-5 could be the cause of the leaky barrier. Claudin-5 is vital for healthy BBB function. Mice lacking claudin-5 have severely compromised and leaky BBB and die shortly after birth

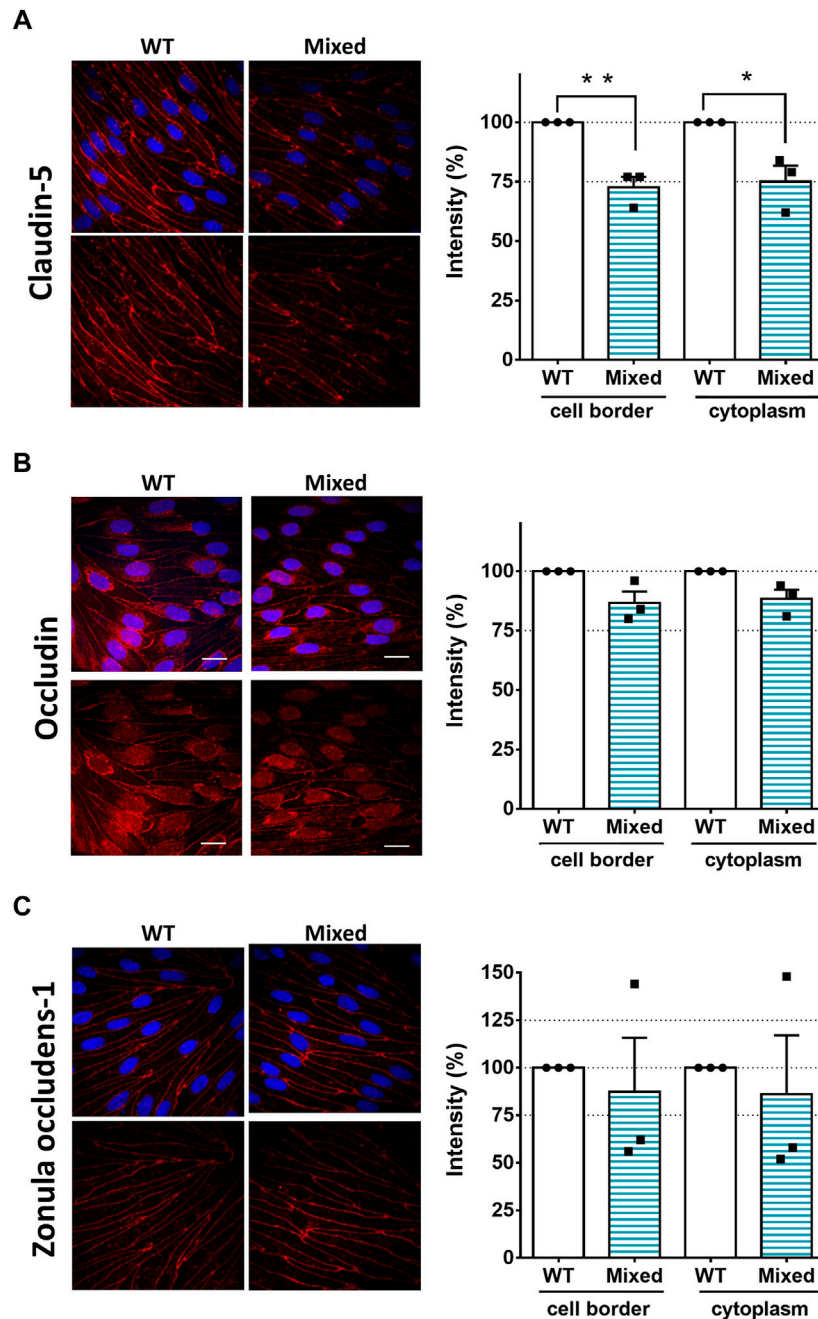


FIGURE 3

SorLA Influences the Tight Junctions of the BECs. (A) Immunocytochemistry and intensity measurement of claudin-5 (B) occludin, (C) and zonula occludens-1. Nuclei are blue, and tight junction proteins are labeled with red. Magnification is $\times 60$. Scale bars are $20 \mu\text{m}$. WT: brain endothelial cells from the wild type -BBB model, Mixed: brain endothelial cells from the mixed-BBB model. Data information: Data are presented as mean \pm SEM $n = 3$ cultures. * $p \leq .05$, ** $p \leq .01$, (Student's t -test).

(Nitta et al., 2003). A disturbance in claudin-5 accompanied by a leaky BBB is a common hallmark of pathological conditions such as Alzheimer's disease (Matsumoto et al., 2020; Zhu et al., 2022). Interestingly, dysfunction and downregulation of SorLA have also been connected to the progression of the disease (Scherzer et al., 2004; Andersen et al., 2016). Namely, SorLA is responsible for the correct sorting of the amyloid precursor protein (Andersen et al., 2005). In this context, it blocks the transport of the protein into compartments that exhibit beta-secretase activity, thus interfering with amyloid- β peptide generation (Andersen et al., 2006). The loss of SorLA

expression accelerates amyloid- β production and senile plaque formation (Dodson et al., 2008). Furthermore, in the familiar form of Alzheimer's disease, a point mutation of SorLA impairs the sorting for degradation of the newly synthesized amyloid- β peptides (Caglayan et al., 2014). Although the deficiency of SorLA accompanied by disturbance of claudin-5 has not been reported so far.

This brief report points out that astrocytes lacking SorLA cause downregulation of claudin-5 in BECs. We focused on the BECs since these cells serve the anatomical basis and form the main barrier of the BBB. The data presented here provide a starting point for future

studies to explore the effect of SorLA in astrocytes on the BBB's integrity. Notably, astrocytes release several factors influencing claudin-5 in BECs during development under healthy and pathological conditions (Alvarez et al., 2013; Broux et al., 2015). The effect of these astrocytic factors on the BBB's integrity would be important to study in connection to the presence or absence of SorLA. SorLA is primarily a sorting receptor, which regulates the homeostasis and vesicular trafficking of numerous substrate proteins (Malik and Willnow, 2020). An important question for future studies is determining how SorLA mediates astrocytic factors' release.

Collectively, the data suggested that SorLA is involved in maintaining the integrity of BBB. The details of the mechanism for this observation are not fully clear. We recommend that the absence of SorLA in astrocytes might affect the junctions of BECs, thereby disturbing the BBB. Our observation represents a powerful new paradigm for understanding neurological disorders that show compromised BBB and SorLA receptor function, such as Alzheimer's disease.

Data availability statement

The original contributions presented in the study are included in the article/Supplementary Materials, further inquiries can be directed to the corresponding authors.

Ethics statement

The animal study was reviewed and approved by the Danish Animal Experiments Inspectorate.

Author contributions

Conceptualization AET and MN; data curation AET; formal analysis AET, and CG; funding acquisition MN; investigation AET,

AK, and DL, CG; methodology AET, and CG; project administration AET and MN; resources MN; supervision, AET, BB, and MN; visualization AET; writing AET, CG, BB, and MN. All authors have read and approved the final manuscript.

Funding

This work has received support from the Research Initiative on Brain Barriers and Drug Delivery funded by the Lundbeck Foundation (Grant no. 2013-14113). The funders had no role in study design, data collection, interpretation, or the decision to submit the work for publication.

Acknowledgments

Annemette B. Marnow is thanked for her expert technical assistance.

Conflict of interest

The authors declare that the research was conducted in the absence of any commercial or financial relationships that could be construed as a potential conflict of interest.

Publisher's note

All claims expressed in this article are solely those of the authors and do not necessarily represent those of their affiliated organizations, or those of the publisher, the editors and the reviewers. Any product that may be evaluated in this article, or claim that may be made by its manufacturer, is not guaranteed or endorsed by the publisher.

References

- Abbott, N. J., Patabendige, A. A., Dolman, D. E., Yusof, S. R., and Begley, D. J. (2010). Structure and function of the blood-brain barrier. *Neurobiol. Dis.* 37 (1), 13–25. doi:10.1016/j.nbd.2009.07.030
- Alvarez, J. I., Katayama, T., and Prat, A. (2013). Glial influence on the blood brain barrier. *Glia* 61 (12), 1939–1958. doi:10.1002/glia.22575
- Andersen, O. M., Reiche, J., Schmidt, V., Gotthardt, M., Spoelgen, R., Behlke, J., et al. (2005). Neuronal sorting protein-related receptor sorLA/LR11 regulates processing of the amyloid precursor protein. *Proc. Natl. Acad. Sci. U. S. A.* 102 (38), 13461–13466. doi:10.1073/pnas.0503689102
- Andersen, O. M., Rudolph, I. M., and Willnow, T. E. (2016). Risk factor SORL1: From genetic association to functional validation in Alzheimer's disease. *Acta Neuropathol.* 132 (5), 653–665. doi:10.1007/s00401-016-1615-4
- Andersen, O. M., Schmidt, V., Spoelgen, R., Gliemann, J., Behlke, J., Galatis, D., et al. (2006). Molecular dissection of the interaction between amyloid precursor protein and its neuronal trafficking receptor SorLA/LR11. *Biochemistry* 45 (8), 2618–2628. doi:10.1021/bi052120v
- Broux, B., Gowing, E., and Prat, A. (2015). Glial regulation of the blood-brain barrier in health and disease. *Semin. Immunopathol.* 37 (6), 577–590. doi:10.1007/s00281-015-0516-2
- Caglayan, S., Takagi-Niidome, S., Liao, F., Carlo, A. S., Schmidt, V., Burgert, T., et al. (2014). Lysosomal sorting of amyloid-beta by the SORLA receptor is impaired by a familial Alzheimer's disease mutation. *Sci. Transl. Med.* 6 (223), 223ra20. doi:10.1126/scitranslmed.3007747
- Cuenco, K. T., Lunetta, K. L., Baldwin, C. T., McKee, A. C., Guo, J., Cupples, L. A., et al. (2008). Association of distinct variants in SORL1 with cerebrovascular and neurodegenerative changes related to Alzheimer disease. *Arch. Neurol.* 65 (12), 1640–1648. doi:10.1001/archneur.65.12.1640
- Dehouck, M. P., Meresse, S., Delorme, P., Fruchart, J. C., and Cecchelli, R. (1990). An easier, reproducible, and mass-production method to study the blood-brain barrier *in vitro*. *J. Neurochem.* 54 (5), 1798–1801. doi:10.1111/j.1471-4159.1990.tb01236.x
- Dodson, S. E., Andersen, O. M., Karmali, V., Fritz, J. J., Cheng, D., Peng, J., et al. (2008). Loss of LR11/SORLA enhances early pathology in a mouse model of amyloidosis: Evidence for a proximal role in Alzheimer's disease. *J. Neurosci.* 28 (48), 12877–12886. doi:10.1523/JNEUROSCI.4582-08.2008
- Fanning, A. S., Jameson, B. J., Jesaitis, L. A., and Anderson, J. M. (1998). The tight junction protein ZO-1 establishes a link between the transmembrane protein occludin and the actin cytoskeleton. *J. Biol. Chem.* 273 (45), 29745–29753. doi:10.1074/jbc.273.45.29745
- Hamm, S., Dehouck, B., Kraus, J., Wolburg-Buchholz, K., Wolburg, H., Risau, W., et al. (2004). Astrocyte mediated modulation of blood-brain barrier permeability does not correlate with a loss of tight junction proteins from the cellular contacts. *Cell Tissue Res.* 315 (2), 157–166. doi:10.1007/s00441-003-0825-y
- Helms, H. C., Abbott, N. J., Burek, M., Cecchelli, R., Couraud, P. O., Deli, M. A., et al. (2016). *In vitro* models of the blood-brain barrier: An overview of commonly used brain endothelial cell culture models and guidelines for their use. *J. Cereb. Blood Flow. Metab.* 36 (5), 862–890. doi:10.1177/0271678X16630991
- Hermans-Borgmeyer, I., Hampe, W., Schinke, B., Methner, A., Nykjaer, A., Susens, U., et al. (1998). Unique expression pattern of a novel mosaic receptor in the developing cerebral cortex. *Mech. Dev.* 70 (1-2), 65–76. doi:10.1016/s0925-4773(97)00177-9

- Itoh, M., Furuse, M., Morita, K., Kubota, K., Saitou, M., and Tsukita, S. (1999). Direct binding of three tight junction-associated MAGUKs, ZO-1, ZO-2, and ZO-3, with the COOH termini of claudins. *J. Cell Biol.* 147 (6), 1351–1363. doi:10.1083/jcb.147.6.1351
- Jacobsen, L., Madsen, P., Jacobsen, C., Nielsen, M. S., Gliemann, J., and Petersen, C. M. (2001). Activation and functional characterization of the mosaic receptor SorLA/LR11. *J. Biol. Chem.* 276 (25), 22788–22796. doi:10.1074/jbc.M100857200
- Jacobsen, L., Madsen, P., Moestrup, S. K., Lund, A. H., Tommerup, N., Nykjaer, A., et al. (1996). Molecular characterization of a novel human hybrid-type receptor that binds the alpha2-macroglobulin receptor-associated protein. *J. Biol. Chem.* 271 (49), 31379–31383. doi:10.1074/jbc.271.49.31379
- Janzer, R. C., and Raff, M. C. (1987). Astrocytes induce blood-brain barrier properties in endothelial cells. *Nature* 325 (6101), 253–257. doi:10.1038/325253a0
- Kanaki, T., Bujo, H., Hirayama, S., Ishii, I., Morisaki, N., Schneider, W. J., et al. (1999). Expression of LR11, a mosaic LDL receptor family member, is markedly increased in atherosclerotic lesions. *Arterioscler. Thromb. Vasc. Biol.* 19 (11), 2687–2695. doi:10.1161/01.atv.19.11.2687
- Kanaki, T., Bujo, H., Hirayama, S., Tanaka, K., Yamazaki, H., Seimiya, K., et al. (1998). Developmental regulation of LR11 expression in murine brain. *DNA Cell Biol.* 17 (8), 647–657. doi:10.1089/dna.1998.17.647
- Klinger, S. C., Glerup, S., Raarup, M. K., Mari, M. C., Nyegaard, M., Koster, G., et al. (2011). SorLA regulates the activity of lipoprotein lipase by intracellular trafficking. *J. Cell Sci.* 124, 1095–1105. doi:10.1242/jcs.072538
- Lochhead, J. J., Yang, J., Ronaldson, P. T., and Davis, T. P. (2020). Structure, function, and regulation of the blood-brain barrier tight junction in central nervous system disorders. *Front. Physiol.* 11, 914. doi:10.3389/fphys.2020.00914
- Madsen, P., Isaksen, T. J., Siupka, P., Toth, A. E., Nyegaard, M., Gustafsen, C., et al. (2019). HSPA12A targets the cytoplasmic domain and affects the trafficking of the Amyloid Precursor Protein receptor SorLA. *Sci. Rep.* 9 (1), 611. doi:10.1038/s41598-018-37336-6
- Malik, A. R., and Willnow, T. E. (2020). VPS10P domain receptors: Sorting out brain health and disease. *Trends Neurosci.* 43 (11), 870–885. doi:10.1016/j.tins.2020.08.003
- Matsumoto, J., Dohgu, S., Takata, F., Iwao, T., Kimura, I., Tomohiro, M., et al. (2020). Serum amyloid A-induced blood-brain barrier dysfunction associated with decreased claudin-5 expression in rat brain endothelial cells and its inhibition by high-density lipoprotein *in vitro*. *Neurosci. Lett.* 738, 135352. doi:10.1016/j.neulet.2020.135352
- Motoi, Y., Aizawa, T., Haga, S., Nakamura, S., Namba, Y., and Ikeda, K. (1999). Neuronal localization of a novel mosaic apolipoprotein E receptor, LR11, in rat and human brain. *Brain Res.* 833 (2), 209–215. doi:10.1016/s0006-8993(99)01542-5
- Nakagawa, S., Deli, M. A., Kawaguchi, H., Shimizudani, T., Shimono, T., Kittel, A., et al. (2009). A new blood-brain barrier model using primary rat brain endothelial cells, pericytes and astrocytes. *Neurochem. Int.* 54 (3-4), 253–263. doi:10.1016/j.neuint.2008.12.002
- Nakagawa, S., Deli, M. A., Nakao, S., Honda, M., Hayashi, K., Nakaoka, R., et al. (2007). Pericytes from brain microvessels strengthen the barrier integrity in primary cultures of rat brain endothelial cells. *Cell Mol. Neurobiol.* 27 (6), 687–694. doi:10.1007/s10571-007-9195-4
- Nielsen, M. S., Gustafsen, C., Madsen, P., Nyegaard, J. R., Hermey, G., Bakke, O., et al. (2007). Sorting by the cytoplasmic domain of the amyloid precursor protein binding receptor SorLA. *Mol. Cell Biol.* 27 (19), 6842–6851. doi:10.1128/MCB.00815-07
- Nitta, T., Hata, M., Gotoh, S., Seo, Y., Sasaki, H., Hashimoto, N., et al. (2003). Size-selective loosening of the blood-brain barrier in claudin-5-deficient mice. *J. Cell Biol.* 161 (3), 653–660. doi:10.1083/jcb.200302070
- Ohtsuki, S., Yamaguchi, H., Katsukura, Y., Asashima, T., and Terasaki, T. (2008). mRNA expression levels of tight junction protein genes in mouse brain capillary endothelial cells highly purified by magnetic cell sorting. *J. Neurochem.* 104 (1), 147–154. doi:10.1111/j.1471-4159.2007.05008.x
- Rubin, L. L., Hall, D. E., Porter, S., Barbu, K., Cannon, C., Horner, H. C., et al. (1991). A cell culture model of the blood-brain barrier. *J. Cell Biol.* 115 (6), 1725–1735. doi:10.1083/jcb.115.6.1725
- Salgado, I. K., Serrano, M., Garcia, J. O., Martinez, N. A., Maldonado, H. M., Baez-Pagan, C. A., et al. (2012). SorLA in glia: Shared subcellular distribution patterns with caveolin-1. *Cell Mol. Neurobiol.* 32 (3), 409–421. doi:10.1007/s10571-011-9771-5
- Scherzer, C. R., Ofte, K., Gearing, M., Rees, H. D., Fang, G., Heilman, C. J., et al. (2004). Loss of apolipoprotein E receptor LR11 in Alzheimer disease. *Arch. Neurol.* 61 (8), 1200–1205. doi:10.1001/archneur.61.8.1200
- Schmidt, V., Schulz, N., Yan, X., Schurmann, A., Kempa, S., Kern, M., et al. (2016). SORLA facilitates insulin receptor signaling in adipocytes and exacerbates obesity. *J. Clin. Invest.* 126 (7), 2706–2720. doi:10.1172/JCI84708
- Schmidt, V., Subkhangulova, A., and Willnow, T. E. (2017). Sorting receptor SORLA: Cellular mechanisms and implications for disease. *Cell Mol. Life Sci.* 74 (8), 1475–1483. doi:10.1007/s00018-016-2410-z
- Srinivasan, B., Kolli, A. R., Esch, M. B., Abaci, H. E., Shuler, M. L., and Hickman, J. J. (2015). TEER measurement techniques for *in vitro* barrier model systems. *J. Lab. Autom.* 20 (2), 107–126. doi:10.1177/2211068214561025
- Stamatovic, S. M., Johnson, A. M., Keep, R. F., and Andjelkovic, A. V. (2016). Junctional proteins of the blood-brain barrier: New insights into function and dysfunction. *Tissue Barriers* 4 (1), e1154641. doi:10.1080/21688370.2016.1154641
- Toth, A. E., Helms, H. C., Harazin, A., Johnsen, K. B., Goldeman, C., Burkhart, A., et al. (2022). Sortilin regulates blood-brain barrier integrity. *FEBS J.* 289 (4), 1062–1079. doi:10.1111/febs.16225
- Toth, A. E., and Nielsen, M. S. (2023). Sortilins in the blood-brain barrier: Impact on barrier integrity. *Neural Regen. Res.* 18 (3), 549–550. doi:10.4103/1673-5374.350197
- Vanlandewijck, M., and Betsholtz, C. (2018a). Single-cell mRNA sequencing of the mouse brain vasculature. *Methods Mol. Biol.* 1846, 309–324. doi:10.1007/978-1-4939-8712-2_21
- Vanlandewijck, M., and Betsholtz, C. (2018b). Vascular single cells. Available at: <http://betsholtzlab.org/VascularSingleCells/database.html>.
- Whittle, A. J., Jiang, M., Peirce, V., Relat, J., Virtue, S., Ebinuma, H., et al. (2015). Soluble LR11/SorLA represses thermogenesis in adipose tissue and correlates with BMI in humans. *Nat. Commun.* 6, 8951. doi:10.1038/ncomms9951
- Willnow, T. E., Petersen, C. M., and Nykjaer, A. (2008). VPS10P-domain receptors - regulators of neuronal viability and function. *Nat. Rev. Neurosci.* 9 (12), 899–909. doi:10.1038/nrn2516
- Yamazaki, H., Bujo, H., Kusunoki, J., Seimiya, K., Kanaki, T., Morisaki, N., et al. (1996). Elements of neural adhesion molecules and a yeast vacuolar protein sorting receptor are present in a novel mammalian low density lipoprotein receptor family member. *J. Biol. Chem.* 271 (40), 24761–24768. doi:10.1074/jbc.271.40.24761
- Youdim, K. A., Avdeef, A., and Abbott, N. J. (2003). *In vitro* trans-monolayer permeability calculations: Often forgotten assumptions. *Drug Discov. Today* 8 (21), 997–1003. doi:10.1016/s1359-6446(03)02873-3
- Zhang, Y., Chen, K., Sloan, S. A., Bennett, M. L., Scholze, A. R., O'Keefe, S., et al. (2014b). An RNA-sequencing transcriptome and splicing database of glia, neurons, and vascular cells of the cerebral cortex. *J. Neurosci.* 34 (36), 11929–11947. doi:10.1523/JNEUROSCI.1860-14.2014
- Zhang, Y., Chen, K., Sloan, S. A., Bennett, M. L., Scholze, A. R., O'Keefe, S., et al. (2014a). Brain RNA-seq. Available at: <http://www.brainrnaseq.org/>.
- Zhang, Y., Sloan, S. A., Clarke, L. E., Caneda, C., Plaza, C. A., Blumenthal, P. D., et al. (2016). Purification and characterization of progenitor and mature human astrocytes reveals transcriptional and functional differences with mouse. *Neuron* 89 (1), 37–53. doi:10.1016/j.neuron.2015.11.013
- Zhu, N., Wei, M., Yuan, L., He, X., Chen, C., Ji, A., et al. (2022). Claudin-5 relieves cognitive decline in Alzheimer's disease mice through suppression of inhibitory GABAergic neurotransmission. *Aging (Albany NY)* 14 (8), 3554–3568. doi:10.18632/aging.204029